Dual Arm Robot Research Report

Analytical Inverse Kinematics Solution for Modularized Dual-Arm Robot With offset at shoulder and wrist

Motivation and Abstract

Generally, an industrial manipulator such as PUMA560 is equipped with 6 degrees of freedom(DoF), it is just enough to reach a position and orientation in 3-D space. However, to achieve dexterous movement like the upper limb of human, different with normal industrial manipulators, such manipulators equipped with 7-DoF kinematic structure is desirable. With the redundant joint, such manipulators may accomplish tasks such as obstacle-avoidance and singularity avoidance while reaching target position at the same time. These tasks are all about manipulator kinematics. However, when one wants to utilize advantages of redundant manipulators, one encounters problem of solving inverse kinematic problem of such manipulators. There is two ways to solve manipulator kinematic problem, one is numerical method and the other is analytical method. Traditionally, it used numerical method to deal with kinematics problem is a traditional way. However, solving Jacobian matrix is rather tedious, not to mention solving its inverse. Also, the relation between joint space and Cartesian space of an arm is not linear, obtaining joint values by numerical method is not satisfactory.

Since that, we develop an analytical inverse kinematic solution for modularized 7-DoF redundant manipulators with offsets at shoulder and wrist and derive analytical inverse kinematic solutions based on different joints as redundnt for it. The manipulator shown in Figure 1 is one of the dual arm robot developed by our laboratory, which is a modularized 7-DoF manipulator with offsets at shoulder and wrist.

Fig. 1 The physical hardware assembly of the modularized 7-DoF manipulator with offsets at shoulder and wrist

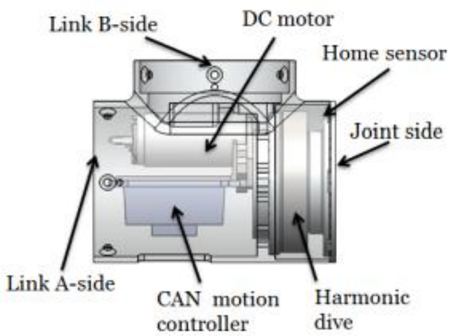

Fig. 2 The modularized component

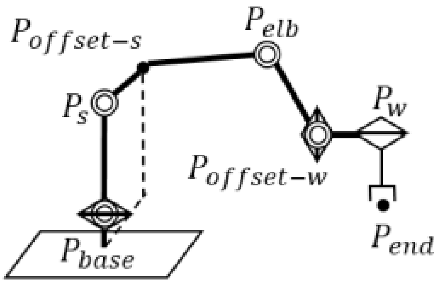

Figure 3: The conceptual structure of the arm

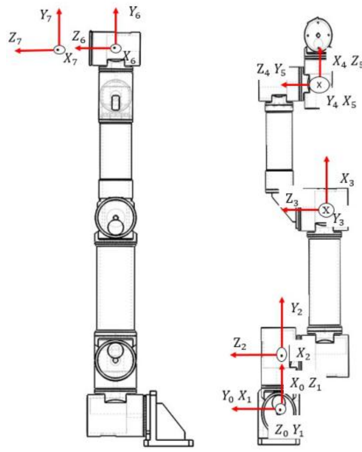

Figure 4: The coordinate system of the arm with offset at shoulder and wrist. The end-effector is not included in this figure

Main Technology

1. Modularized component

Parts of the proposed arm where motors, controller, reduction gear, and others installed are modularized component, as shown in Figure 2. In addition, links can be attached to this part at Link A-side and Link B-side of this modularized component. Also, there is a window for direct access to each controller during maintenance. Generally, the modularized design grants it advantages in easy assembly.

2. Analytical inverse kinematic equation

As shown in Figure 3, since there are offsets in shoulder and wrist, we cannot apply fixed-arm-angle method. Hence, we have to use fixed-joint method. Firstly, we make derivation with joint 1 value regarded as redundancy parameter. Then, solution with value of joint 2 seen as redundancy parameter will be solved afterwards.

In the following sections, we denote $A^{a}_{b,c=d}$ as a value A of a referred to frame b, while a specified value c is d. Also, as shown in Figure 3 and Figure 4, the origin of frame 0 and 1 are at P_b, but they have different orientation. The origin of frame 2 is at P_s, while the origin of frame 3 is at P_e. The origin of frame 4 and 5 are at $P_{offset-w}$ with different orientation. Lastly, the origin of frame 6 and 7 are at P_w and P_{end} respectively.

DENAVIT HARTENBERG PARAMETERS

Joint	θ(rad)	α(rad)	a(m)	d(m)	θ_{min}(°)	θ_{max}(°)
1	$\theta_1+\pi/2$	$\pi/2$	0	0	−90	90
2	$\theta_2+\pi/2$	$\pi/2$	0.131	0	−90	90
3	$\theta_3+\pi/2$	0	−0.131	0.350	−80	80
4	θ_4	0	0	0.301	−90	0
5	$\theta_5+\pi/2$	$\pi/2$	0	0	−90	90
6	$\theta_6+\pi/2$	$\pi/2$	0.115	0	-90^{+}	90^{-}
7	$\theta_7+\pi/2$	$\pi/2$	0.120	0	−180	180

Table 1. DH parameters

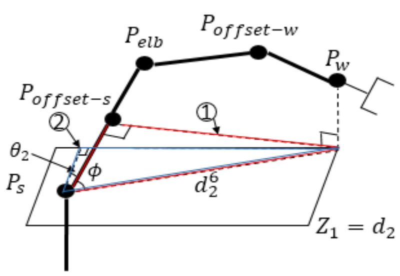

Figure 5: The projection triangle used to solve θ_2

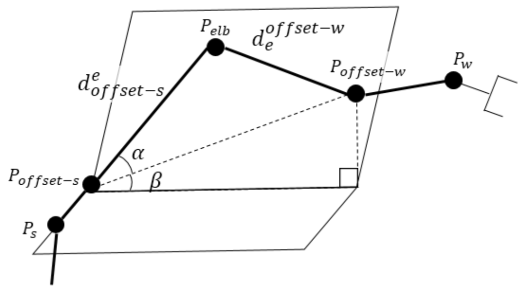

Figure 6: The triangle spanned by $\mathrm{P_{offset-w}}$, $\mathrm{P_e}$, and $\mathrm{P_{offset-s}}$

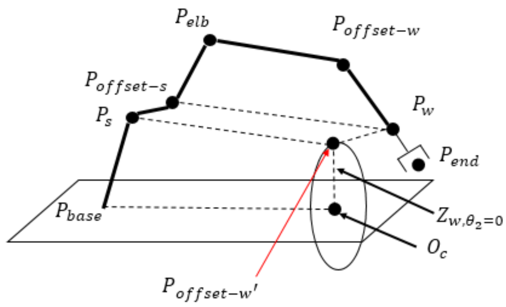

Figure 7: The trajectory of virtual offset-wrist forms a circle when all joints are fixed except joint 1

A. CLOSED-FORM KINEMATIC EQUATIONS WITH JOINT 1 AS REDUNDANT JOINT

With the knowledge of $\mathrm{R_0^7}$ and $\mathrm{P_0^7}$, we obtain wrist position, $\mathrm{P_0^6}$:

$$\begin{cases} P_0^6 = P_0^7 + R_0^7 v_7^6 \\ v_7^6 = \begin{bmatrix} 0 & 0 & -d_7 \end{bmatrix}^T \end{cases} \quad (4)$$

where $\mathrm{V_7^6}$ is the vector from end-effector position to the wrist position. Next, because θ_1 is known, we are able to solve the position of the shoulder, P_0^2:

$$P_0^2 = \begin{bmatrix} d_2\cos\theta_1 & d_2\sin\theta_1 & 0 \end{bmatrix}^T \quad (5)$$

then also with the knowledge of θ_1, we can transform both P_0^2 and P_0^6 into P_1^2 and P_1^6:

$$\begin{cases} P_1^2 = R_0^{1^T} P_0^2 \\ P_1^6 = R_0^{1^T} P_0^6 \end{cases} \quad (6)$$

Next, find $P_{1,z=d_2}^2$, i.e. project P_1^6 to $Z_1 = d_2$. As Figure 5 shows, then we can find θ_2 with the aid of projection triangle 1 and 2:

$$\begin{cases} \phi = atan2(\sqrt{d_{26}^2 - d_3^2}) \\ \theta_2 = atan2(\mathrm{Y}_{1,z=d_2}^6, X_{1,z=d_2}^6) - \phi \end{cases} \quad (7)$$

where ϕ is an angle of triangle 1. $\mathrm{d_{26}}$ indicates the distance from P_1^2 to $P_{1,z=d_2}^6$. So far we obtain θ_1 and θ_2, now we can solve θ_6 and θ_7 by the following equation:

$$R = R_2^7 = R_0^{2^T} R_0^7 \quad (8)$$

$$R = \begin{bmatrix} \cdots & \cdots & \cdots \\ \cdots & \cdots & \cdots \\ -\cos\theta_6\cos\theta_7 & \cos\theta_6\sin\theta_7 & -\sin\theta_6 \end{bmatrix} \quad (9)$$

$$\begin{cases} \theta_6 = atan2(-R_{3,3}, \sqrt{R_{3,1}{}^2 + R_{3,2}{}^2}) \\ \theta_7 = atan2(-R_{3,2}, R3,1) + \pi \end{cases} \quad (10)$$

where $\mathrm{R_{i,j}}$ is the value in $\mathrm{i^{th}}$ row, $\mathrm{j^{th}}$ column of matrix R. In this step, since we already know θ_1, θ_2, θ_6, and θ_7,

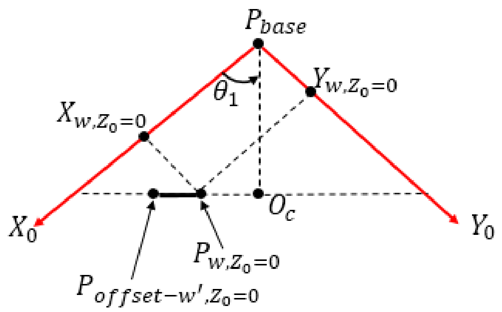

Figure 8: Projection of the redundancy circle on plane $Z_0 = 0$

we know $P_{offset-s}$ and $P_{offset-w}$:

$$\begin{cases} T = T_2^5 = T_2^1 T_1^0 T_0^7 T_7^6 T_6^5 \\ P_{offset-w} = P_2^5 = \begin{bmatrix} T_{1,4} & T_{2,4} & T_{3,4} \end{bmatrix}^T \end{cases} \quad (11)$$

$$P_2^{offset} = \begin{bmatrix} 0 & 0 & -d_3 \end{bmatrix}^T \quad (12)$$

Next, with the help of projection triangle on the plane $Z_2 = -d_3$., which is spanned by $P_{offset-s}$, P_e, and $P_{offset-w}$, , we can find θ_3 and θ_4:

$$\begin{cases} \cos\theta_4 = \dfrac{{d^3_{offset-s}}^2 + {d_3^5}^2 - {d^5_{offset-s}}^2}{2 \times d_3^5 \times d^3_{offset-s}} \\ \theta_4 = atan2(\sqrt{1 - \cos{\theta_4}^2}, \cos\theta_4) \end{cases} \quad (13)$$

$$\begin{cases} \alpha = \dfrac{{d^3_{offset-s}}^2 + {d^5_{offset-s}}^2 - {d_3^5}^2}{2 \times d^3_{offset-s} \times d^5_{offset-s}} \\ \beta = atan2(Y_2^5, X_2^5) \\ \theta_3 = \alpha + \beta - \pi/2 \end{cases} \quad (14)$$

where $d^3_{offset-s}$ is a_3 and d_3^5 is a_4 as in Table 1, $d^5_{offset-s}$ can be obtained by simple Euclidean norm calculation.

Now only θ_5 remains unknown. It can be found with the information of all the other joint value and R_0^7:

$$R = R_4^5 = {R_0^4}^T R_0^7 {R_5^7}^T \quad (15)$$

$$R = \begin{bmatrix} \cos\theta_5 + \pi/2 & \dots & \dots \\ \sin\theta_5 + \pi/2 & \dots & \dots \\ 0 & \dots & \dots \end{bmatrix} \quad (16)$$

$$\theta_5 = atan2(R_{2,1}, R_{1,1}) - \pi/2 \quad (17)$$

Finally, we find all the joint value by the aforementioned equations using fixed-joint method in joint 1 is regarded as redundant parameter.

B. CLOSED-FORM KINEMATIC EQUATIONS WITH JOINT 1 AS REDUNDANT JOINT

Since joint 1 and joint 2 can exchange with each other in assembly, that indicates that joint 1 and joint 2 have similar influence on end-effector position and orientation. Thus, to make the analytical equation for this type of arm more complete, we also find equations when joint 2 value is redundancy parameter. When we know joint 1 value, $P_{offset-s}$ can be easily found, then we can find joint 2 value as (6) and(7) did. However, with the circle drawn by trajectory of P_w when all the joints are fixed except for joint 1, we are able to find θ_1 based on known θ_2, then applying from (8) to (17) so as to find all values of all other joints.

As shown in Figure 7, P_w is on the circle whose center is O_C. Based on our coordinate system construction shown in Figure 4, we consider the offset from P_s to $P_{offset-s}$ between frame 2 and 3. However, we can define a virtual point $P_{offset-w'}$ where $d^{w}_{offset-w'}$ is the same as $d^{offset-s}_{s}$, and $|d_3|$. After defining virtual offset-wrist $P_{offset-w'}$, we can find the distance between O_C and P_b, $d_0^{O_C}$:

$$\begin{cases} Z^{w}_{0,\theta_2=0} = Z^{6}_{0,\theta_2=0} = (Z^6_0 - d_3 \sin\theta_2)/\cos\theta_2 \\ d_0^{offset-w'} = \sqrt{d_0^{6^2} - d_3^{\ 2}} \end{cases} \quad (18)$$

$$d_0^{O_c} = \sqrt{d_0^{offset-w'^2} - Z^{w\ \ 2}_{0,\theta_2=0}} \quad (19)$$

where $Z^2_{0,\theta_2=0}$ is the radius of the circle and $d_0^{offset-w'}$ is the distance from virtual offset-wrist to base. Next,

we are able to find value of joint 1 with the projection shown in Figure 8:

$$d_0^{O_c} = Y_{w,Z_0=0} \sin\theta_1 + X_{w,Z_0=0} \cos\theta_1 \quad (20)$$

$\sin\theta_1$ and $\cos\theta_1$ can be represented by a quadratic from equation where $\tan\frac{\theta_1}{2}$ is the parameter.

then by rearranging (20) into a quadratic equation, such that we can find two solutions of θ_1. We then check both of the candidates by equations from (4) to (7) to find out which one is correct.

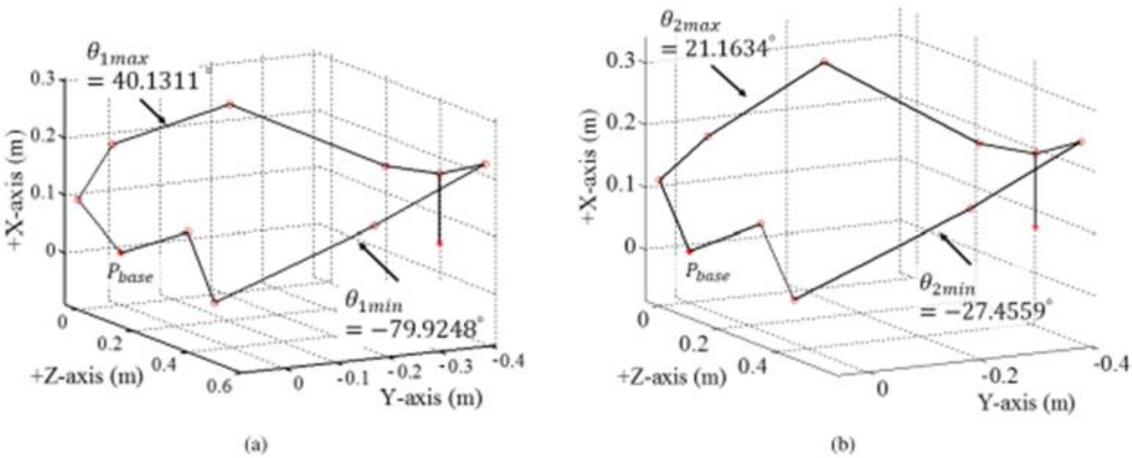

Figure 9. Extreme posture of manipulator for the acceptable joint value. In (a), θ_1 is redundant and in (b), θ_2 is redundant, where the tip position and orientation are specified by (23) and (24).

Experiment Result

To verify the correctness of the proposed equations, simulations are implemented as follows. The verification is implemented by applying the kinematic equations on the custom-made manipulator with offsets at shoulder and wrist. The arm can be seen at Figure 1. In addition, the coordinate construction is the same as shown in Figure 4. Though all the joints can rotate 360° freely in most of the time, after concerning the environment, we should assume that there are limitations for every joints. The limitations are shown in Table I. Assume the desired position of the end-effector is:

$$^{d_1}P_0^7 = \begin{bmatrix} 0.1 & -0.3 & 0.6 \end{bmatrix}^T \qquad (23)$$

$$^{d_1}R_0^7 = \begin{bmatrix} 0 & 0 & -1 \\ 0 & 1 & 0 \\ 1 & 0 & 0 \end{bmatrix} \qquad (24)$$

we check both sets of equations where θ_1 is treated as redundancy parameter and θ_2 is treated as redundancy parameter. In figure 9(a), while θ_1 is maximum, the joint value set is as the following:

$$\{40.1311^\circ, 21.0410^\circ, -79.9999^\circ, -47.5916^\circ, 20.7521^\circ, -36.9819^\circ, 116.7087^\circ\}$$

In contrast, while θ_1 is minimum, the joint value set is as the following:

$$\{-79.9248^\circ, -27.4559^\circ, -54.7635^\circ, -14.1619^\circ, -89.9995^\circ, 60.8894^\circ, 18.6079^\circ\}$$

As shown in figure 9(b), while θ_2 is maximum, the joint value set is as the following:

$$\{24.6492^\circ, 21.1634^\circ, -67.1780^\circ, -53.8042^\circ, 21.5756^\circ, -22.8881^\circ, 113.0717^\circ\}$$

n contrast, while θ_2 is minimum, the joint value set is as the following:

$$\{-76.6303^\circ, -27.4559^\circ, -50.5157^\circ, -20.8797^\circ, -81.3340^\circ, 59.6911^\circ, 23.9906^\circ\}$$

We can check the joint value solved by proposed analytical inverse kinematics equations by performing forward kinematic, then we confirm that the proposed equations are correct.

Future application

By deriving analytical inverse kinematics solution for the modularized 7-DoF redundant manipulator, we may solve the kinematics faster and more precisely. Also, with the newly-designed modularized component for all joint part where motors installed, we may assemble the arm in a simpler way.